1-4-2012

New Lithium Measurements in Metal-Poor Stars

Marc Schaeuble
Clemson University

Jeremy R. King
Clemson University, jking2@clemson.edu

Follow this and additional works at: https://tigerprints.clemson.edu/physastro_pubs

New Lithium Measurements in Metal-Poor Stars[†]

Marc Schaeuble & Jeremy R. King

Department of Physics and Astronomy, Clemson University, Clemson, SC 29630-0978

`marcs944@gmail.com,jking2@clemson.edu`

ABSTRACT

We provide λ6708 Li I measurements in 37 metal-poor stars, most of which are poorly-studied or have no previous measurements, from high-resolution and high-S/N spectroscopy obtained with the McDonald Observatory 2.1m and 2.7m telescopes. The typical line strength and abundance uncertainties, confirmed by the thinness of the Spite plateau manifested by our data and by comparison with previous measurements, are ≤ 4 mÅ and $\leq 0.07 - 0.10$ dex respectively. Two rare moderately metal-poor solar-$T_{\rm eff}$ dwarfs, HIP 36491 and 40613, with significantly depleted but still detectable Li are identified; future light element determinations in the more heavily depleted HIP 40613 may provide constraints on the Li depletion mechanism acting in this star. We note two moderately metal-poor and slightly evolved stars, HIP 105888 and G265-39, that appear to be analogs of the low-Li moderately metal-poor subgiant HD 201889. Preliminary abundance analysis of G 265-39 finds no abnormalities that suggest the low Li content is associated with AGB mass-transfer or deep mixing and p-capture. We also detect line doubling in HIP 4754, heretofore classified as SB1.

Subject headings: Stars

1. INTRODUCTION

The discovery of near-constant Li abundances in warm little-evolved metal-poor stars by Spite & Spite (1982) quickly spawned a vigorous cottage industry seeking to derive the

---

[†]This paper includes data taken at The McDonald Observatory of The University of Texas at Austin.

cosmological baryonic density under the assumption that the Li abundances in such stars reflect the product of Big Bang nucleosynthesis. While WMAP observations (Dunkley et al. 2009) have obviated the use of light element abundances to provide precision cosmological parameters, the study of metal-poor stellar Li abundances still has considerable import. Even recent studies with warmer metal-poor T_{eff} scales, which result in higher Li abundances *ceteris paribus*, find that stellar estimates of the primordial Li abundance is a factor of 3 smaller than that suggested by WMAP-based baryonic densities (Hosford et al. 2010). The adequacy of our understanding of Big Bang nucleosynthesis remains unclear given this discrepancy.

A salient question in considering this discrepancy is the degree to which metal-poor stellar Li abundances are post-primordial–i.e., possibly afflicted by stellar depletion, Galactic enrichment, or both. Indeed, evidence exists that the Li abundances in the most metal-poor warm little-evolved stars is not constant, but declines with declining [Fe/H] (Sbordone et al. 2010). While standard stellar models predict little, if any, stellar Li depletion in such stars, observational evidence suggests that such models suffer deficiencies in explaining Li abundances in cool metal-poor dwarfs and evolved metal-poor stars (Pilachowski, Sneden & Booth 1993; Ryan & Deliyannis 1995).

Determination of Li abundances in large samples of metal-poor stars of various evolutionary state, mass, and metallicity are needed to provide the context in which to understand the relation of those abundances with the primordial value. Large samples also yield rare examples of stars with anomalous light element abundances that can provide constraints on Galactic enrichment and stellar depletion processes (King et al. 1996; Ryan & Deliyannis 1995; Boesgaard 2007; Koch, Lind & Rich 2011). Here, we make a modest contribution to expanding the size of such samples by providing Li measurements based on high-resolution spectroscopy in 37 metal-poor stars. Our stars were selected from our existing observations connected with unrelated programs, and are metal-poor objects from the surveys of Carney et al. (1994) and Ryan & Norris (1991) that have kinematics hotter than evinced by thin disk stars. The stars selected are also poorly-studied with respect to light element abundances; the majority have no previous Li measurements.

2. OBSERVATIONAL DATA

Spectra were obtained during observing runs in January and August 1994 and October 2004 with the McDonald Observatory 2.7-m Harlan J. Smith Telescope and its 2dcoude spectrograph (Tull et al. 1995), and in February and September 1994 with the McDonald Observatory 2.1-m Otto Struve Telescope and its Sandiford Cassegrain Echelle Spectrograph

(McCarthy et al. 1993). The nominal spectral resolution is $R\sim60,000$, except for the January 1994 2.7-m observations for which smaller slits and pre-Textronix CCDs with smaller pixels yielded resolutions of 67,000-90,000. The per pixel S/N in the $\lambda6708$ Li I region ranges from 80-450, and is in the smaller range 150-200 for most stars. The echelle package within IRAF[1] was used to perform standard reductions including bias subtraction, flat fielding, order tracing and summation, and wavelength calibration to Th-Ar lamp spectra. Examples of the spectroscopic data can be seen in Figure 1. The stars considered here are listed in Table 1; select cross-identifications are listed in the final column.

Fig1
Tab1

3. ABUNDANCE ANALYSIS AND UNCERTAINTIES

3.1. General Approach

While most metal-poor star Li abundance studies are conducted using measured line strengths, our preference is to fit realistic models of the data (i.e., synthetic spectra) to the data and report the equivalent widths associated with these model fits. Synthetic spectra were calculated in LTE using an updated version of MOOG (Sneden 1973) and the $\lambda6708$ Li I region linelist from King et al. (1997) modified using more recent laboratory-based atomic data from VALD (Kupka et al. 1999), semi-empirical atomic data from Kurucz[2], and the molecular CN data of Mandell, Ge & Murray (2004). We utilized model atmospheres interpolated within ATLAS9 grids[3] that correspond to the stellar parameters described next.

3.2. Stellar Parameters

Inasmuch as our main goal is fitting model spectra to the data in order to determine a line strength (rather than an abundance per se) that reflects the absorption flux, accurate stellar parameters are of little consequence. In principle, the parameters could have a second order influence due to curve of growth effects and the presence of blending (primarily CN for the $\lambda6708$ Li I feature at our resolution and given the small macroscopic line broadening associated with our stars). However, even these second order effects are negligible: the

---

[1]IRAF is distributed by the National Optical Astronomy Observatories, which are operated by the Association of Universities for Research in Astronomy, Inc., under cooperative agreement with the National Science Foundation.

[2]http://kurucz.harvard.edu/linelists.html

[3]http://kurucz.harvard.edu/grids.html

weakness of the Li I feature and the distribution of its absorbed flux over multiple hyperfine components nulls the curve of growth effects, and the metal-poverty of our stars nulls blending effects (especially so for diatomic CN blends). While adopted stellar parameters need only be reasonably plausible for the purpose of measuring line strengths via model profile fits, it should be said that accurate stellar parameters are certainly required to determine reliable abundances from the syntheses. These parameter-dependent abundances enable us to empirically examine our claimed estimated uncertainties by examining abundance scatter, compare our results with those of others, and identify any stars with anomalous Li abundances that may provide additional insight into metal-poor stellar Li depletion or Galactic or stellar Li production.

The parameters were estimated through extant literature data as described below. Even for the poorly-studied stars, color-based $T_{\rm eff}$ estimates on modern IRFM-based scales are easily determined, metallicity estimates from low-resolution spectroscopic measurements are available, and gravities can be determined using isochrones and information about evolutionary status from HIPPARCOS parallaxes and/or Stromgren photometry. The proof of the relative quality of the parameters (most importantly $T_{\rm eff}$ for the Li abundance determinations) will be found in the pudding of the abundance results shown in Figure 3, which evinces only small scatter (± 0.07 dex) about the visible Spite plateau at warm $T_{\rm eff}$.

3.2.1. Effective Temperature

Effective temperatures were estimated using four primary sources: excitation balance-based results from spectroscopic fine analyses in the literature (unavailable for many of our objects), Balmer line fitting-based results in the literature, the color-based values from Carney et al. (1994), Alonso & Martinez-Roger (1996), and Casagrande et al. (2010). For a few stars, original color-based estimates were made using the new new color-$T_{\rm eff}$ calibrations of Casagrande et al. (2010); in those cases, appropriate reddening corrections were applied using the appropriate transformations from Schlegel, Finkbeiner, & Davis (1998) and extinctions or reddenings taken from Schuster et al. (2006), Schuster & Nissen (1989), and/or Carney et al. (1994). Mean $T_{\rm eff}$ values, uncertainties in those means, and corresponding references are given in columns 2 and 3 of Table 1. Uncertainties based on one source are taken from the source, while those based on 2 sources are simply the difference between the source values.

3.2.2. Gravity

Gravities were estimated from high-resolution spectroscopic fine analyses and/or Yale-Yonsei isochrones (Demarque et al. 2004) based on our $T_{\rm eff}$ value and/or M_V inferred from HIPPARCOS parallax measurements or Stromgren calibrations. In the former case, log g is in general double-valued depending on whether the star is on the main-sequence or subgiant branch. Such ambiguities were cleanly resolved based on the HIPPARCOS- and Stromgren-based M_V values with only a few exceptions:

G16-20: The spectroscopic gravity derived by Nissen & Schuster (2010) and that adopted on the basis of catalog-based distance and isochrone-based mass by Reddy & Lambert (2008) differ by a factor of 20, making it unclear whether this star is a dwarf or warm subgiant. The Stromgren photometry of Schuster, Parrao & Contreras Martinez (1993) suggests the star is a subgiant given its placement in the c_1 versus $(b-y)$ classification diagram of Schuster et al. (2004). However, the extensive efforts of Arnadottir, Feltzing & Lundstrom (2010) to identify Stromgren-based evolutionary discriminants suggest that distinguishing between dwarfs and subgiants at $(b-y){\leq}0.55$ (which holds for G 16-20) on the basis of Stromgren photometry cannot be done reliably. We assume subgiant status.

G130-65: The log g values inferred from $T_{\rm eff}$ and the Carney et al. (1994) distance (which assumes dwarf status) are in considerably better agreement than the subgiant-like log g values inferred from the $T_{\rm eff}$ and the Schuster et al. (2006) Stromgren-based M_V. We assume dwarf status.

G265-39: Given the negligible HIPPARCOS parallax, we assume subgiant status in estimating the gravity of this star from isochrones and our adopted $T_{\rm eff}$ value. The so-derived log g value also yields good agreement between Fe abundances derived from Fe I and Fe II lines; moreover, abundances of Ba and Y derived from gravity-sensitive singly ionized lines are in good agreement with similarly metal-poor stars analyzed in Edvardsson et al. (1993). Details can be found in §4.

Notes concerning the gravity estimates of a few other stars are made in Table 1. In those cases, we believe that dwarf/subgiant status is clearly resolved. The gravity estimates and associated references/notes can be found in columns 4 and 5 of Table 1. Those stars with multiple log g estimates, from both spectroscopic fine analyses and parallaxes/isochrones, suggest that the log g estimates are good to within $0.10 - 0.15$ dex; regardless, the Li line strengths and abundances are insensitive to the adopted log g values. The 15 stars with Hipparcos parallaxes $\geq$2 their parallax uncertainties are plotted in the H-R diagram of Figure 2 with a selection of Yale-Yonsei isochrones (Demarque et al. 2004) for context.   Fig2

3.2.3.   Metallicity and Microturbulence

Metallicity estimates from the literature and their references are given in columns 6 and 7 of Table 1. Mean uncertainties are determined as they were for the $T_{\rm eff}$ values. For metallicities coming from the Carney et al. (1994)estimates alone, the uncertainties are internal values based on their measurements from multiple spectra. For stars with measurements from multiple independent sources, comparison of metallicity estimates suggests $0.15 - 0.2$ dex as a more realistic mean uncertainty for the Carney et al. (1994) values alone. Microturbulence has negligible influence on the derived abundances and inferred line strengths. In the interest of full disclosure, columns 8 and 9 list the values we adopted and their origin.

3.3.   Results and Uncertainties

Our object spectra are narrow-lined, showing no discernible signatures of rotation-dominated profiles. The synthetic spectra were smoothed to account for instrumental and thermal (and any small rotational) broadening by convolution with a Gaussian. The FWHM used in the smoothing was empirically determined for each star by direct measurement of weak metal lines throughout the spectra, fits to the $\lambda6717$ Ca I feature, and fits to the metal lines in the $\lambda6104$ Li I region using the linelist of King et al. (2010). Examples of the synthetic fits to the spectra can be seen in Figure 1. The resulting LTE Li abundances are listed in column 10 of Table 1. The equivalent widths corresponding to the best fit synthetic profiles, as determined from traditional residual minimization compared to the observed data over the line profile, are given in column 11 of Table 1. NLTE abundance corrections (which do not impact the line strength measurements) were taken from Carlsson et al. (1994) and applied to the LTE abundances; the resulting NLTE abundances are listed in column 12 of Table 1.

Uncertainties in the LTE Li abundances are dominated by uncertainties in the smoothing, continuum placement, fitting, and $T_{\rm eff}$ estimates. Uncertainties in metallicity (including the direct effect of blending), gravities, and microturbulence are negligible for the $\lambda6708$ Li I line in our stars. The effects of uncertainties in our measurements of smoothing, our choice of continuum normalization, and our $T_{\rm eff}$ estimate (given in column 2 of Table 1) on the derived abundances were measured by refitting syntheses accordingly adjusted; the abundance uncertainties are attached to the LTE abundances in Table 1. Sources of uncertainty in the line strength are those listed above excluding those for $T_{\rm eff}$; these amount to a 10-15% uncertainty in the reported line strengths.

Notes are made concerning two of the objects in our sample:

HIP4754: Latham et al. (2002) classify HIP 4754 as a single-lined spectroscopic binary with a 347 day period. In our spectrum, the lines consistently evince a very weak blue asymmetry that can be seen in the $\lambda 6708$ Li I feature in Figure 1. This asymmetry is confirmed in Fourier space: the cross-correlation function (CCF) formed from HIP 4754 and other warm stars in our sample (utilized as templates) shows a weak but distinct blue hump. Fitting the CCFs with a two-component Gaussian indicates the radial velocity separation in our spectrum is ~ 5 km s^{-1}.

G130-65: The red wing of the Li I feature appears to exhibit an absorption asymmetry not seen in other lines (see Figure 1). Our fit to the profile ignores this asymmetry. Additional spectroscopy would be desirable to confirm the presence or absence of a real asymmetry and any association with ^{6}Li. We note that the asymmetry in the profile of HIP 36491 seen in Figure 1 is simply the ^{7}Li hyperfine structure, which is manifest for this object due to the higher spectral resolution used when observing this star.

4. DISCUSSION

The main product provided here is the line strengths contained in column 11 of Table 1, which can be utilized in future homogenized meta-analyses of Li in metal-poor stars. A few remarks concerning the results can be made with the help of Figure 3, which plots the derived abundances versus $T_{\rm eff}$. Metal-poor ([Fe/H]≤ -1.29) dwarfs or mildly-evolved subgiants are shown as solid squares; more metal-rich ($-0.92 \leq$[Fe/H]≤ -0.44) dwarfs or little-evolved subgiants are shown as open squares. Cooler, more highly-evolved subgiants and giants ($T_{\rm eff} \leq 5576$ K, log $g \leq 3.77$) are shown as open circles. Fig3

4.1. The Spite Plateau and Quality Estimates

The metal-poor dwarfs evince the well-known pattern of near constant Li abundance for $T_{\rm eff} \geq 5700$ K, referred to as the "Spite plateau" after Spite & Spite (1982), and declining Li abundance at cooler $T_{\rm eff}$ due to standard stellar model Li burning during the pre-main-sequence and main-sequence with the proportion of each being $T_{\rm eff}$- (or, more accurately, mass) dependent (Deliyannis, Demarque & Kawaler 1990), and the probable effects of rotationally-induced mixing (Ryan & Deliyannis 1995). The scatter in Li on the metal-poor Spite plateau provides information about the quality of our results. We confine our attention to the metal-poor dwarfs with $T_{\rm eff} \geq 5692$ K in order to avoid the effects of the most significant depletion. We fit these data with a 2nd order polynomial that is shown as the dashed

line in Figure 1. The data exhibit a scatter of only 0.070 dex around this fit. The larger expected value of 0.099 dex, based on the uncertainties in Table 1, suggests we may have overestimated the latter. Inasmuch as we believe the T_{eff} and fitting uncertainties have been realistically estimated, this indicates the subjectively assessed uncertainties in continuum normalization and smoothing are overestimated. The uncertainties in T_{eff} in Table 1 lead to an estimate of an expected abundance scatter of 0.062 dex. Subtracting this in quadrature from the observed scatter implies the line strengths uncertainties (which are controlled by uncertainties in fitting, continuum normalization, and smoothing) are $\leq 8\%$– translating to an equivalent width uncertainty of $\leq$2-4 mÅ.

An alternative estimate of the line strength uncertainties is provided by comparison of our measurements with the eleven previous measurements in the notes to Table 1. The standard deviation of the differences between our line strength differences and those of others is ± 5.4 mÅ (the average difference, in the sense of our measures minus others', is -2.6 mÅ). Assuming equivalent uncertainties in our measurements and others' implies a typical uncertainty in our measurements of ± 3.8 mÅ–in good accord with the Spite plateau-based estimate.

Our mean Spite plateau abundance of $\log N(\mathrm{Li}) \sim 2.3$ agrees with numerous other measures of similarly warm and metal-poor stars. We do not address here the pregnant issue of the inconsistency of such a primordial Li abundance inferred from stellar measurements with that implied by WMAP observations for two reasons. First, the absolute T_{eff} scale of metal-poor stars remains uncertain, perhaps by as much as 100-200 K (King 1993; Casagrande et al. 2010; Hosford et al. 2010), especially for stars with [Fe/H]≤ -2; this scale has significant implications for the primordial Li abundance derived from metal-poor stars (King 1994; Melendez & Ramirez 2004). Second, the Li abundance in the warmest little-evolved halo stars may decline with decreasing metallicity at ultra-low metallicites– behavior predicted by Ryan et al. (1999), observed by Sbordone et al. (2010), but disputed by Melendez et al. (2010). Whether the Spite plateau is in fact a plateau at very low [Fe/H] remains uncertain. However, we simply note that the slope of our Spite plateau stars' NLTE Li abundances with [Fe/H], 0.14$\pm$0.05 dex/dex, is in good agreement with the value (0.15$\pm$0.05) derived by Hosford et al. (2009) for main-sequence stars in the metallicity range $-3.3 \leq$[Fe/H]≤ -2.3 using temperatures derived from Fe excitation under the LTE assumption, and with the value (0.14$\pm$0.12) derived by Hosford et al. (2010) using temperatures derived from Fe excitation in a NLTE framework ignoring H collisions.

4.2.   The Warm Moderately Metal-Poor Dwarfs

The four more moderately metal-poor ($-0.92 \leq$[Fe/H]≤ -0.44) dwarfs evince a real factor of $\sim$7 scatter in their Li abundance. From a theoretical perspective, such a spread can naturally be accommodated by the inclusion of rotationally-induced mixing (with or without an age spread) in stellar models. Figures 4 and 5 of Pinsonneault, Deliyannis & Demarque (1992) show that such models produce a wider dispersion in pre-main-sequence and main-sequence depletion compared to more metal-poor models. From an observational context, the situation is more complex and interesting. Nearly all field dwarfs with near-solar T_{eff} values in the metallicity range above have Li abundances of $\sim$2.1 with modest scatter ($\sim$0.2 dex), as seen in Figure 2 of Lambert, Heath & Edvardsson (1991). Stars with significantly lower abundances (like HIP 36491 and 40613 in our sample) appear to be very rare, as seen in Figure 2 of Lambert, Heath & Edvardsson (1991).

What is interesting about our measurements of HIP 36491 and 40613 is that they reveal Li to be more heavily depleted in these stars but still detectable. As described in detail in §5.1 of Stephens et al. (1997), observations of Be in such stars can place constraints on numerous candidate mechanisms responsible for the Li depletion in these objects. The Be abundance derived by Smiljanic et al. (2009) places HIP 36491 just above the mean Galactic Be-Fe trend at our metallicity in both their Figure 10 as well as in Figure 2 of the independent study of Boesgaard et al. (2010). Any Be depletion in this star is apparently limited to $\leq$0.1 dex if one compares the abundance to the upper envelope of the Smiljanic et al. (2009) and Boesgaard et al. (2010) Be-Fe data. The inequality of inferred Li and Be depletion, $\sim$0.4 dex versus $\sim$0 dex, would seem to exclude diffusion as a causal mechanism. The relative depletions are qualitatively consistent with mass loss, gravity waves, meridional circulation, and rotationally-induced mixing. Determination of the Be abundance in the more highly Li-depleted HIP 40613 would be of interest in perhaps providing stronger constraints on these remaining depletion mechanisms.

4.3.   The Evolved Stars

The Li abundances of the 5 subgiants and giants with $T_{eff} \leq$5600 K are lower than the Spite plateau values, and consistent with the values expected from non-diffusive dilution (e.g. Figure 8 of Pilachowski, Sneden & Booth 1993) that occurs when the stellar surface convection zone dips into deeper hotter Li-depleted regions. The two more metal-rich ([Fe/H]~ -0.7) subgiants with $T_{eff} \geq$5700 K, HIP 105888 and G 265-39, show Li abundances significantly lower than the trend formed by the other subgiants and the aforementioned dilution models. These two stars are reminiscent of HD 201889, a subgiant with similar

T_{eff} and [Fe/H] that also demonstrates a rare anomalously low Li abundance compared with other warm subgiants at this T_{eff} in Figure 7 of Pilachowski, Sneden & Booth (1993).

A possible explanation for the low Li abundances in HIP 105888 and G 265-39 is an environmental origin– perhaps these stars were contaminated with the Li-depleted products of a former AGB companion or have undergone unexpected p-capture processing and deep mixing that have destroyed Li and brought this Li depleted material to the surface. The first possibility might lead to s-process enhancements, while the second possibility might also be accompanied by Ne→Na and O→N cycling. We have conducted a preliminary search for these signatures in G 265-39, but failed to find them.

We measured the line strengths of a few Fe I, Fe II, O I, Na I, Zr II, Y II, and Ba II lines in G 265-39 and a daytime sky (solar proxy) spectrum acquired with the McDonald 2.7-m. The lines, line strengths, and resulting absolute logarithmic number abundances derived from the line strengths using MOOG are listed in Table 2. Atomic data is taken from Edvardsson et al. (1993), King et al. (1998), and Schuler et al. (2006). The mean Fe abundance from the 5 lines is [Fe/H]= −0.73, which is in outstanding agreement with the value adopted in Table 1 (−0.71) within the mean measurement uncertainty (±0.05 dex) alone. Because of the particular sensitivities of the individual lines, the complementary ratios [O I,Zr II, Y II, Ba II/Fe II] and [Na I/Fe I] are essentially free of uncertainties in the stellar parameters (at least compared to measurement uncertainties). The ratios[4] in G 265-39 are similar to those exhibited by stars of the same [Fe/H] in Figure 15 of Edvardsson et al. (1993). In particular, O does not appear underabundant nor does Na appear overabundant as might occur if our star was contaminated by material having undergone O→N and Ne→Na cycling and deep mixing (either *in situ* or from a former AGB companion); nor is there any indication of an n-capture element overabundance that might accompany contamination by material from a former AGB companion.

More extensive surveys of metal-poor stars are needed to identify larger numbers of objects with anomalous Li abundances. Subsequent or accompanying determination of abundances of a suite of elements in these stars is needed to understand what information they provide about the effects of stellar physics and Galactic chemical evolution on Li abundances. Coupled with a solid theoretical framework, such data will be required to establish the existence or not of a decline of stellar Li at extremely low metallicities and to place the current apparent mismatch of these Li abundances with WMAP results into an appropriate cosmological context.

---

[4]Our permitted O I-based ratio was placed on $\lambda 6300$ forbidden O I-based scale of Edvardsson et al. (1993) using their equation 11.

REFERENCES

Allen, C., Poveda, A., & Herrera, M. A. 2000, A&A, 356, 529

Alonso, A., & Martinez-Roger, C. 1996, A&AS, 117, 227

Arnadottir, A. S., Feltzing, S., & Lundstrom, I. 2010, A&A, 521, 40

Axer, M., Fuhrmann, K., & Gehren, T. 1994, A&A, 291, 895

Beers, T. C., Rossi, S., Norris, J. E., Ryan, S. G., & Shefler, T. 1999, AJ, 117, 981

Bensby, T., Feltzing, S., Lundstroem, I., & Ilyin, I. 2005, A&A, 433, 185

Boesgaard, A. M., Stephens, A., & Deliyannis, C. P. 2005, ApJ, 633, 398

Boesgaard, A. M. 2007, ApJ, 667, 1196

Boesgaard, A. M., Rich, J. A., Levesque, E. M., & Bowler, B. P. 2010, IAUS, 268, 231

Caffau, E.; Bonifacio, P.; Faraggiana, R.; Franois, P.; Gratton, R. G.; Barbieri, M. 2005, A&A, 441, 533

Carlsson, M., Rutten, R. J., Bruls, J. H. M. J., & Shchukina, N. G. 1994, A&A, 288, 860

Carney, B. W., Latham, D. W., Laird, J. B., & Aguilar, L. A. 1994, AJ, 107, 2240

Carney, B. W., Wright, J. S., Sneden, C., Laird, J. B., Aguilar, L. A., & Latham, D. W. 1997, AJ, 114, 363

Casagrande, L., Ramirez, I., Melendez, J., Bessell, M., & Asplund, M. 2010, A&A, 512, 54

Cavallo, R. M., Pilachowski, C. A., & Rebolo, R. 1997, PASP, 109, 226

Cenarro, A. J., Peletier, R. F., Sanchez-Blazquez, P., Selam, S. O., Toloba, E., Cardiel, N., Falcon-Barroso, J., Gorgas, J., Jimenez-Vicente, J., & Vazdekis, A. 2007, MNRAS, 374, 664

Clementini, G., Gratton, R. G., Carretta, E., & Sneden, C. 1999, MNRAS, 302, 22

Deliyannis, C. P., Demarque, P., & Kawaler, S. D. 1990, ApJS, 73, 21

Demarque, P., Woo, J.-H., Kim, Y.-C., & Yi., S. K. 2004, ApJS, 155, 667

Dunkley, J., Komatsu, E., Nolta, M. R., Spergel, D. N., Larson, D., Hinshaw, G., Page, L., Bennett, C. L., et al. 2009, ApJS, 180, 306

Edvardsson, B., Andersen, J., Gustafsson, B., Lambert, D. L., Nissen, P. E., & Tomkin, J. 1993, A&A, 275, 101

Fuhrmann, K. 1998, A&A, 338, 161

Fulbright, J. P. 2000, AJ, 120, 1841

Goldberg, D., Mazeh, T., Latham, D. W., Stefanik, R. P., Carney, B. W., & Laird, J. B. 2002, AJ, 124, 1132

Gratton, R. G., Carretta, E., & Castelli, F. 1996, A&A, 314, 191

Gratton, R. G., Sneden, C., Carretta, E., & Bragaglia, A. 2000, A&A, 354, 169

Gratton, R. G., Carretta, E., Claudi, R., Lucatello, S., & Barbieri, M. 2003, A&A, 404, 187

Gutierrez, C. M., Garcia Lopez, R. J., Rebolo, R., Martin, E. L., & Francois, P. 1999, A&AS, 137, 93

Horch, E. P., Robinson, S. E., Meyer, R. D., van Altena, W. F., Ninkov, Z., & Piterman, A. 2002, AJ, 123, 3442

Hosford, A., Ryan, S. G., Garcia Perez, A. E., Norris, J. E., & Olive, K. A. 2009, A&A, 493, 601

Hosford, A., Garcia Perez, A. E., Collet, R., Ryan, S. G., Norris, J. E., & Olive, K. A. 2010, A&A, 511, 47

Ivans, I. I., Sneden, C., James, C. R., Preston, G. W., Fulbright, J. P., Hoeflich, P. A., Carney, B. W., & Wheeler, J. C. 2003, ApJ, 592, 906

Ishigaki, M., Chiba, M., & Aoki, W. 2010, PASJ, 62, 143

James, C. R. 2000, Ph. D. dissertation, U. Texas Austin

Jones, J. B., Wyse, R. F. G., & Gilmore, G. 1995, PASP, 107, 632

Jonsell, K., Edvardsson, B., Gustafsson, B., Magain, P., Nissen, P. E., & Asplund, M. 2005, A&A, 440, 321

King, J. R., Schuler, S. C., Hobbs, L. M., & Pinsonneault, M. H. 2010, ApJ, 710, 1610

King, J. R., 1993, AJ, 106, 1206

King, J. R. 1994, AJ, 107, 1165

King, J. R., Deliyannis, C. P., & Boesgaard, A. M. 1996, AJ, 112, 2839

King, J. R., Deliyannis, C. P., Hiltgen, D. D., Stephens, A., Cunha, K., & Boesgaard, A. M. 1997, AJ, 113, 1871

King, J. R., Stephens, A., Boesgaard, A. M., & Deliyannis, C. P. 1998, AJ, 115, 666

Koch, A., Lind, K., & Rich, R. M. 2011, ApJ, 738, L29

Kupka, F., Piskunov, N., Ryabchikova, T. A., Stempels, H. C., & Weiss, W. W. 1999, A&AS, 138, 119

Lambert, D. L., Heath, J. E., & Edvardsson, B. 1991, MNRAS, 253, 610

Latham, D. W., Stefanik, R. P., Torres, G., Davis, R. J., Mazeh, T., Carney, B. W., Laird, J. B., & Morse, J. A. 2002, AJ, 124, 1144

Lejeune, Th., Cuisinier, F., & Buser, R. 1998, A&AS, 130, 65

Mandell, A. M., Ge, J., & Murray, N. 2004, AJ, 127, 1147

McCarthy, J. K., Sandiford, B. A., Boyd, D., & Booth, J. 1993, PASP, 105, 881

Melendez, J., & Ramirez, I. 2004, ApJ, 615, L33

Melendez, J., Casagrande, L., Ramirez, I., Asplund, M., & Schuster, W. J. 2010, A&A, 515, L3

Mishenina, T. V., Korotin, S. A., Klochkova, V. G., & Panchuk, V. E. 2000, A&A, 353, 978

Mishenina, T. V., & Kovtyukh, V. V. 2001, A&A, 370, 951

Nissen, P. E.; Chen, Y. Q.; Asplund, M; Pettini, M. 2004, A&A, 415, 993

Nissen, P. E., Akerman, C., Asplund, M., Fabbian, D., Kerber, F., Kaeufl, H. U., & Pettini, M. 2007, A&A, 469, 319

Nissen, P. E., & Schuster, W. J. 2010, A&A, 511, 10

Pilachowski, C. A., Sneden, C., & Booth, J. 1993, ApJ, 407, 699

Pinsonneault, M. H., Deliyannis, C. P., & Demarque, P. 1992, ApJS, 78, 179

Rastegaev, D. A., Balega, Yu. Yu., & Malogolovets, E. V. 2007, AstBu, 62, 235

Rebolo, R., Beckman, J. E., & Molaro, P. 1988, A&A, 192, 192

Ramirez, I., Allende Prieto, C., & Lambert, D. L. 2007, A&A, 465, 271

Reddy, B. E., Lambert, D. L., & Prieto, C. A. 2006, MNRAS, 367, 1329

Reddy, B. E., & Lambert, D. L. 2008, MNRAS, 391, 95

Ryan, S. G., & Norris, J. E. 1991, AJ, 101, 1865

Ryan, S. G., & Deliyannis, C. P. 1995, ApJ, 453, 819

Ryan, S. G., Norris, J. E., Beers, T. C., 1999, ApJ, 523, 654

Sbordone, L, Bonifacio, P., Caffau, E., Ludwig, H.-G., Behara, N. T., Gonzalez Hernando, J. I., Steffen, M., Cayrel, R., et al. 2010, A&A, 522, A26

Schlegel, D. J., Finkbeiner, D. P., & Davis, M. 1998, ApJ, 500, 525

Schuler, S. C., King, J. R., Terndrup, D. M., Pinsonneault, M. H., Murray, N., & Hobbs, L. M. 2006, ApJ, 636, 432

Schuster, W. J., & Nissen, P. E. 1989, A&A, 222, 69

Schuster, W. J., Parrao, L., & Contreras Martinez, M. E. 1993, A&AS, 97, 951

Schuster, W. J., Beers, T. C., Michel, R., Nissen, P. E., & Garca, G. 2004, A&A, 422, 527

Schuster, W. J., Moitinho, A., Marquez, A., Parrao, L., & Covarrubias, E. 2006, A&A, 445, 939

Shi, J. R., Gehren, T., Zhang, H. W., Zeng, J. L., & Zhao, G. 2007, A&A, 465, 587

Simmerer, J., Sneden, C., Cowan, J. J., Collier, J., Woolf, V. M., & Lawler, J. E. 2004, ApJ, 617, 1091

Smiljanic, R., Pasquini, L., Bonifacio, P., Galli, D., Gratton, R. G., Randich, S., & Wolff, B. 2009, A&A, 499, 103

Sneden, C. 1973, ApJ, 184, 839

Sousa, S. G., Santos, N. C., Israelian, G., Lovis, C., Mayor, M., Silva, P. B., & Udry, S. 2005, A&A, 526, 99

Spite, M., & Spite, F. 1982, Nature, 297, 483

Stephens, A., Boesgaard, A. M., King, J. R., & Deliyannis, C. P. 1997, ApJ, 491, 339

Stephens, A., & Boesgaard, A. M. 2002, AJ, 123, 1647

Tomkin, J., Lemke, M., Lambert, D. L., & Sneden, C. 1992, AJ, 104, 1568

Tull, R. G., MacQueen, P. J., Sneden, C., & Lambert, D. L. 1995, PASP, 107, 251

Valenti, J. A., & Fischer, D. A. 2005, ApJS, 159, 141

White, R. J., Gabor, J. M., & Hillenbrand, L. A. 2007, aj, 133, 2524

Yong, D., & Lambert, D. L. 2003, PASP, 115, 22

Zhang, L., Ishigaki, M., Aoki, W., Zhao, G., & Chiba, M. 2009, ApJ, 706, 1095

Zhang, H. W., & Zhao, G. 2006, A&A, 449, 127

Zhang, H. W., & Zhao, G. 2005, MNRAS, 364, 712

Zhang, H.-W, & Zhao, G. 2003, ChJAA, 3, 453
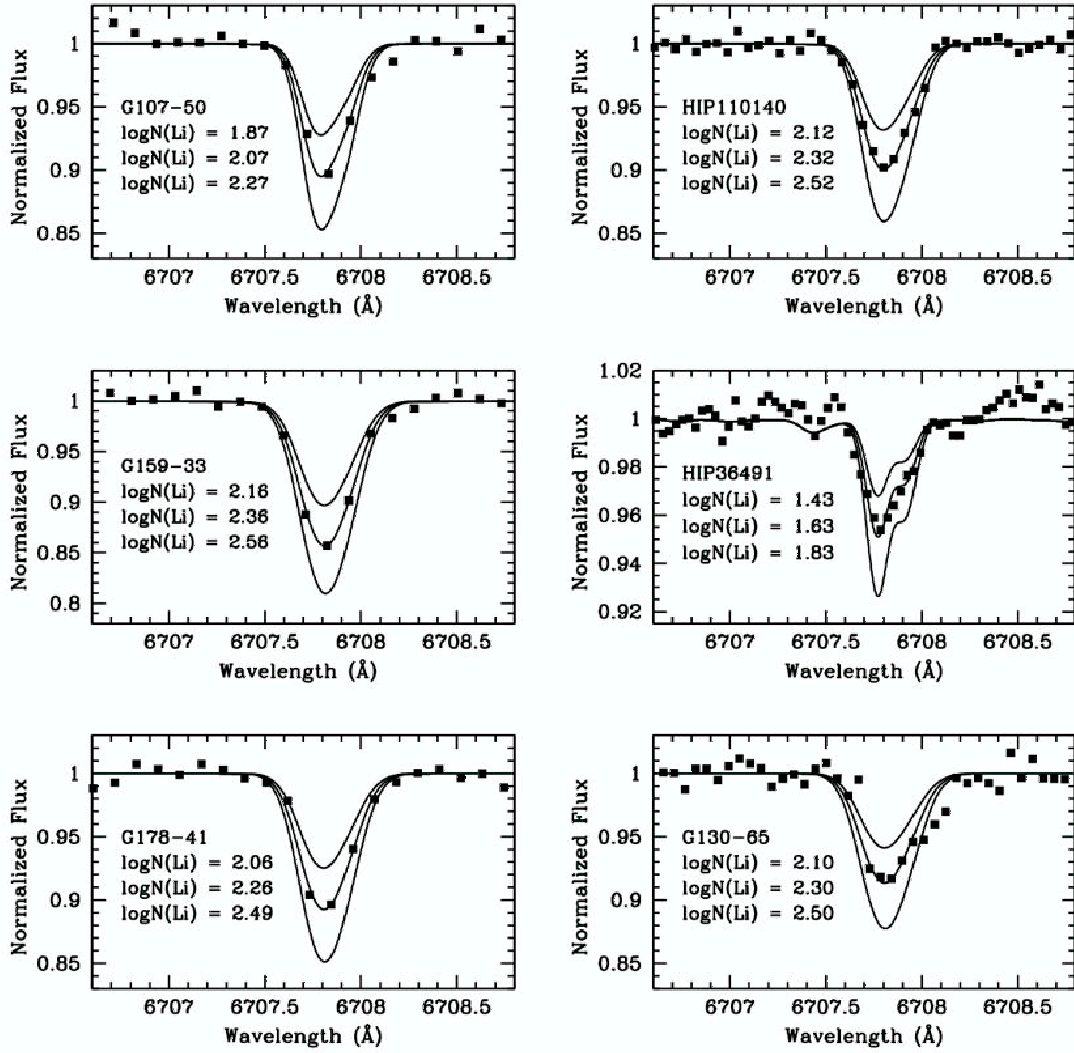
Fig. 1.— Sample $\lambda 6708$ Li I region data (solid points) and syntheses (lines) with input Li abundances stepped by 0.2 dex.
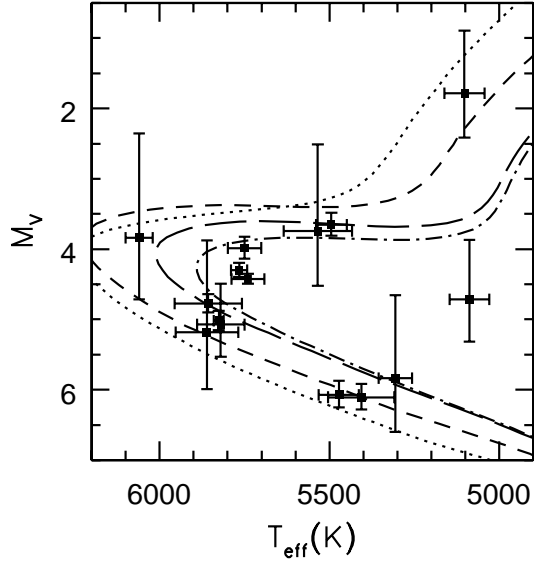
Fig. 2.— Our sample tars having Hipparcos parallaxes satisfiying $\pi/\sigma_\pi \geq 2$ in an H-R diagram using Hipparcos-based absolute magnitude and our effective temperatures; error bars reflect 1σ level uncertainties in the parallaxes and $T_{\rm eff}$ values. Several Yale-Yonsei $[\alpha/\text{Fe}]= +0.3$ isochrones are shown for reference: $[\text{Fe/H}]= -1.5$, 12 Gyr (short dashed line); $[\text{Fe/H}]= -0.9$, 8 Gyr (medium dashed line); $[\text{Fe/H}]= -0.5$, 8 Gyr (long dashed line); and $[\text{Fe/H}]= -0.5$, 10 Gyr (dot-dashed lined).

Fig. 3.— Our synthesis-based NLTE Li abundances are plotted versus $T_{\rm eff}$. Filled squares are metal-poor ([Fe/H]≤-1.26) dwarfs or warm little-evolved subgiants. Open squares indicate more metal-rich ($-0.92\leq$[Fe/H]≤-0.44) dwarfs. Open circles designate subgiants or giants with $T_{\rm eff}\leq5600$ K.

Table 1.   Metal-Poor Sample and Parameters

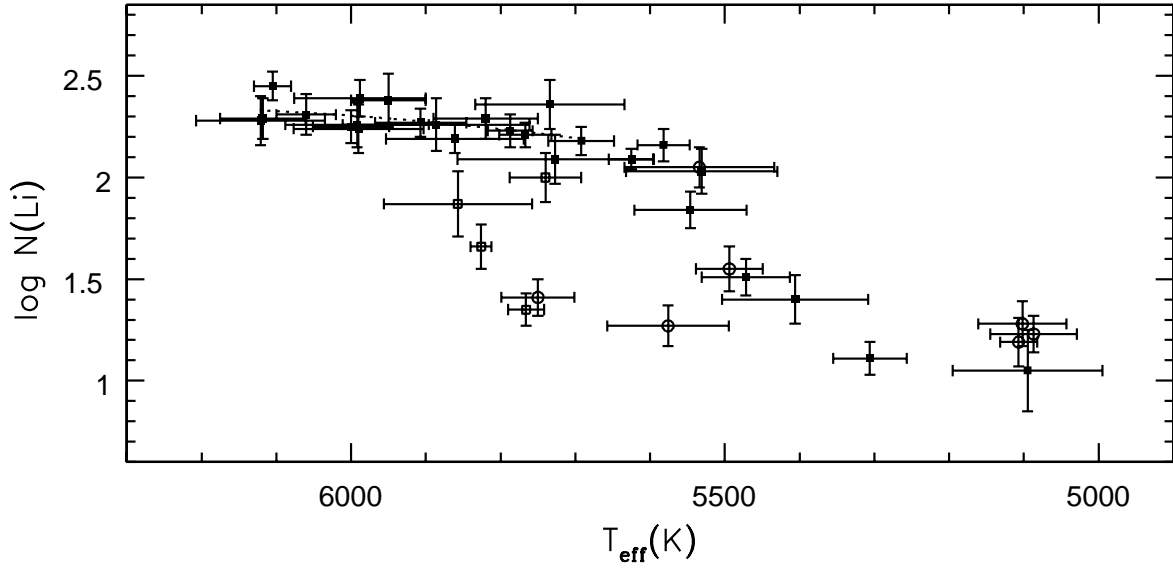| Name	$T_{\rm eff}$ K	Ref	$\log g$ cgs	Ref	[Fe/H]	Ref	ξ km/s	Ref	A(Li) LTE	EEW mÅ	A N
G158-30	5546±75	1	4.50	1	−1.29±0.07	1	0.4	1	1.79±0.09	23.4	1
G130-65	6121±86	3,4	4.50	5	−2.33±0.03	3	1.4	6	2.30±0.12	28.1	2
HIP4754	5534±100	8	3.50	9	−1.72±0.10	8	1.5	6	1.99±0.10	35.3	2
G2-38	5950±50	11	4.57	11	−1.29±0.06	11	1.3	6	2.39±0.13	39.0	2
G172-58	6118±57	3,8,13	4.38	14	−1.57±0.25	3,8,13	1.4	6	2.31±0.10	28.4	2
G133-45	5767±35	3,16	4.57	5	−1.50±0.03	3	1.2	6	2.20±0.06	36.5	2
G159-33	5734±100	8	4.63	5	−1.54±0.10	8	1.2	6	2.36±0.12	48.8	2
HIP12710	6000±51	11,17,18,19	4.26	11,17,18,19	−1.83±0.13	11,17,18,19	1.40	11,18,19	2.26±0.08	30.0	2
G36-47	5907±61	3	4.55	5	−1.63±0.14	3,21	1.3	6	2.27±0.07	33.8	2
G95-11	5531±101	3	4.70	5	−2.09±0.05	3	1.1	6	2.00±0.11	35.4	2
G37-37	5990±87	1	3.76	1	−2.36±0.06	1	1.55	1	2.24±0.12	30.0	2
G191-55	5787±30	3,13,23	4.54	5,13,23	−1.74±0.12	3,13,23	1.2	13,23	2.23±0.08	37.1	2
G107-50	5727±131	3	4.63	5	−2.25±0.03	3	1.2	6	2.07±0.12	30.6	2
HIP36491	5826±14	11,3,4,25	4.41	11,26,25	−0.92±0.03	11,3,27,25,28,29,30	1.3	11,27,25,28	1.63±0.11	10.8	1
G234-24	5988±88	3,4	4.47	5	−1.60±0.04	3	1.3	6	2.41±0.09	38.9	2
HIP40613	5766±24	3,4,32,33,34	4.29	26,32,34,35	−0.58±0.02	3,36,37,32,33,34,35	1.3	6	1.32±0.08	6.9	1
HIP45069	6105±25	39,40	3.87	39,40	−1.41±0.05	39,40	1.40	39,40	2.47±0.07	34.1	2
HIP47316	5992±96	3,4,16	4.47	6	−1.57±0.05	3,41	1.3	6	2.27±0.11	30.7	2
HIP49371	5102±59	11,4,25,32	2.66	11,25,32,42	−1.83±0.06	11,25,32,43,44,45,42	1.6	4,25,32,45	1.13±0.11	15.0	1
HIP63100	5861±92	3,4	4.57	5	−1.78±0.11	3,46	1.3	6	2.19±0.07	31.6	2
G150-50	5095±100	3	4.77	5	−1.85±0.03	3	1.0	6	0.95±0.20	10.5	1

Table 1—Continued

Name	$T_{\rm eff}$ K	Ref	$\log g$ cgs	Ref	[Fe/H]	Ref	ξ km/s	Ref	A(Li) LTE
G178-41	5886±125	3,4	4.58	5	−2.29±0.16	3,4,48	1.3	b	2.26±0.13
HIP74588	5107±25	23,39	3.21	23,39	−1.28±0.04	23,39	1.3	23,39	1.05±0.12
G16-20	5625±30	50	3.64	50	−1.42±0.04	50	1.5	50	2.04±0.05
G168-26	5582±35	3	4.65	5	−1.80±0.04	3	1.1	6	2.14±0.08
HIP85757	5494±45	3,4,25	3.77	25,26	−0.71±0.05	3,36,27,25,29,37	1.5	6	1.48±0.11
HIP97747	5087±58	4,51,52	2.85	53,51,52,54	−1.51±0.05	23,51,52,54	1.5	6	1.08±0.09
G265-39	5576±81	3,4	3.77	26,56	−0.71±0.05	3	1.5	6	1.21±0.10
HIP103269	5472±59	11,3,4,25,57	4.67	11,5	−1.72±0.03	11,3,21,58,27,25,57	1.1	11,27,25,57	1.45±0.09
HIP105488	5820±70	3,8	4.52	5	−1.48±0.14	3,8,21	1.3	6	2.29±0.10
HIP105888	5750±49	11,3,4,27,60,25,57	4.01	11,26	−0.74±0.05	11,3,27,60,25,57,28,29	1.5	6	1.37±0.09
HIP106924	5406±98	8,3,58,27,62	4.70	5,63	−1.84±0.08	8,3,58,27,62	1.1	6	1.34±0.12
G214-5	5692±44	3	4.60	5	−1.91±0.22	3,21	1.2	6	2.17±0.07
HIP110140	6060±40	50,3,4,64	4.00	5	−1.50±0.04	50,3,64,65,66	1.5	50,65	2.32±0.10
HIP111332	5857±99	3,4	4.42	26	−0.44±0.04	3,21	1.3	6	1.85±0.16
HIP116259	5740±48	3,4	4.42	26	−0.55±0.03	3	1.2	6	1.97±0.12
HIP117150	5306±49	3	4.69	5	−1.62±0.05	3	1.1	6	1.03±0.08

References. —

(1) Stephens & Boesgaard (2002)

(2) A(Li)= 1.59, EW(Li)= 16.5±1.0 Boesgaard, Stephens & Deliyannis (2005)

(3) Carney et al. (1994)

(4) Casagrande et al. (2010)

(5) Estimated from 12 Gyr [α/Fe]= +0.3 Yale-Yonsei isochrones (Demarque et al. 2004) with Lejeune et al. (1998)
status of Carney et al. (1994) and/or M_V value of Schuster et al. (2006) and/or the HIPPARCOS-based parallax

(6) adopted here

(7) The Yale-Yonsei dwarf-like log g values inferred from $T_{\rm eff}$ and distance are in considerably better agreement
Schuster et al. (2006) M_V values. We thus assume dwarf evolutionary status and adopt the Carney et al. (1994)

(8) Reddy & Lambert (2008)

(9) Estimated from 12 Gyr [α/Fe]= +0.3 Yale-Yonsei isochrones (Demarque et al. 2004) with Lejeune et al. (1
giant/dwarf status inferred by Reddy & Lambert (2008)

(10) SB 1 with $P = 347$d,$e = 0.38$ according to Latham et al. (2002); the double-lined nature of the star is detec

(11) Axer, Fuhrmann & Gehren (1994)

(12) Binary with 25 arcsec separation and 5.5 photographic magnitude brightness difference (Allen, Poveda & H

(14) The log g value of Reddy & Lambert (2008) is 0.5 dex larger than that implied for their spectroscopic $T_{\rm eff}$
from our $T_{\rm eff}$ value assuming dwarf status implied by the results of Reddy & Lambert (2008) and Zhang & Zhao

(15) Zhang & Zhao (2003) find EW(Li)= 37.4 mÅ, A(Li)= 2.20

(16) Alonso & Martinez-Roger (1996)

(17) Cenarro et al. (2007)

(18) Ivans et al. (2003)

(19) James (2000)

(20) Ivans et al. (2003) find EW(Li)=32.7 mÅ, A(Li)= 2.35

(21) Schuster et al. (2006)

(22) Boesgaard, Stephens & Deliyannis (2005) find $A(Li) = 2.28$, EW(Li)= 34.5±1.4

(23) Simmerer et al. (2004)

(24) Binary with 0.8 arcsec separation and 2 photographic magnitude brightness difference resolved by speckle
Fulbright (2000)

(26) Gravity estimated from our adopted $T_{\rm eff}$ and/or HIPPARCOS-based M_V value using an 8 Gyr Yale-Yonsei

(27) Gratton et al. (2003)

(28) Zhang & Zhao (2006)

(29) Clementini et al. (1999)

(30) Jonesell et al. (2005)

(31) Fulbright (2000) finds EW(Li)= 13.0, A(Li)= 1.70

(32) Gratton, Carretta & Castelli (1996)

(33) Bensby et al. (2005)

(34) Sousa et al. (2011)

(35) Edvardsson et al. (1993)

(36) Ramirez, Allende Prieto & Lambert, D. L. (2007)

(37) Reddy, Lambert & Prieto (2006)

(38) The $T_{\rm eff}$ and log g values of Axer, Fuhrmann & Gehren (1994) are 200 K hotter and $\geq$0.7 dex smaller tha
not utilize their values here. (39) Zhang et al. (2009)

(40) Ishigaki, Chiba & Aoki (2010)

(41) Schuster & Nissen (1989)

(42) Tomkin et al. (1992)

(43) Pilachowski, Sneden & Booth (1993)

(44) Cavallo, Pilachowski & Rebolo (1997)

(45) Gratton et al. (2000)

(46) Beers et al. (1999)

(47) $T_{\rm eff}$ uncertainty is adopted

(48) Ryan & Norris (1991)

(49) The HIPPARCOS parallax and spectroscopic gravity estimates indicate the dwarf status inferred from Car

(50) Nissen & Schuster (2010)

(51) Carney et al. (1997)

(52) Yong & Lambert (2003)

(53) Gravity estimated from both our adopted T_{eff} and/or the HIPPARCOS-based M_V value using the 12 Gyr Y

(54) Jones, Wyse & Gilmore (1995)

(55) Carney et al. (1997) find EW(Li)= 11.2 mÅ, A(Li)= 0.89±0.15

(56) The low Li and negligible parallax suggest subgiant status.

(57) Mishenina & Kovtyukh (2001)

(58) Valenti & Fischer (2005)

(59) Fulbright (2000) finds EW(Li)= 16.0, A(Li)= 1.34; Shi et al. (2007) find A(Li)= 1.60 (60) Fuhrmann (1998)

(61) Fulbright (2000) finds EW(Li)= 7.9 mÅ, A(Li) = 1.37; (Gutierrez et al. 1999) find EW(Li)< 13 mÅ

(62) Mishenina et al. (2000)

(63) The spectroscopic gravity of Valenti & Fischer (2005) is a factor of 2.5 smaller than that implied by the Yale value implied by our adopted T_{eff} and the HIPPARCOS-based M_V value.

(64) Nissen et al. (2007)

(65) Nissen et al. (2004)

(66) Caffau et al. (2005)

(67) Rebolo, Beckman & Molaro (1988) fine EW(Li)= 37 mÅ, $A(li) = 2.24$

(68) Latham et al. (2002) find SB1 with $P = 6083\mathrm{d}, e = 0.52$; Horch et al. (2002) used speckle interferometry to

(69) Gutierrez et al. (1999) find EW(Li)= 26 mÅ; White, Gabor & Hillenbrand (2007) find EW(Li)= 37 mÅ

Table 2.   Abundances in G 265-39

Species	λ Å	χ eV	$\log gf$	EW$_\odot$ mÅ	$\log N_\odot$	EW$_\star$ mÅ	$\log N_\star$
O I	7771.95	9.15	$+0.369$	74.0	8.92	53.7	8.57
O I	7774.17	9.15	$+0.223$	62.7	8.89	43.8	8.54
O I	7775.39	9.15	$+0.001$	52.6	8.93	35.9	8.59
Na I	6154.22	2.10	-1.61	39.8	6.36	19.5	5.88
Na I	6160.75	2.10	-1.31	60.0	6.34	33.1	5.87
Fe I	5141.75	2.42	-2.19	94.3	7.59	69.7	6.79
Fe I	6151.62	2.18	-3.33	52.5	7.53	32.2	6.88
Fe I	6173.34	2.22	-2.90	70.2	7.49	53.6	6.89
Fe II	6149.23	3.89	-2.80	38.0	7.59	24.0	6.86
Fe II	5100.66	2.81	-4.13	20.3	7.47	8.7	6.61
Y II	5087.43	1.08	-0.36	48.7	2.31	31.7	1.36
Zr II	5112.27	1.66	-0.76	10.0	2.64	2.3	1.49
Ba II	6141.73	0.70	-0.077	127.9	2.49	94.6	1.36